Proceedings of the 4th International Conference on Civil Engineering for Sustainable Development (ICCESD 2018), 9~11 February 2018, KUET, Khulna, Bangladesh (ISBN-978-984-34-3502-6)

EFFECT OF INTERPARTICLE FRICTION ON THE SMALL STRAIN STIFFNESS OF GRANULAR MATERIALS BY DEM

Md. M Sazzad[1] and Md. S Islam[2]

[1] *Professor, Department of Civil Engineering, Rajshahi University of Engineering & Technology, Bangladesh, e-mail: mmsruet@gmail.com*
[2] *Undergraduate Student, Department of Civil Engineering, Rajshahi University of Engineering & Technology, Bangladesh, e-mail: sharif.ruet12@gmail.com*

ABSTRACT

Interparticle friction plays a crucial role in the stability of granular materials such as sand during shear. In this study, the effect of interparticle friction angle at a very small strain level (less than 0.001% strain) is examined using the Discrete Element Method (DEM). DEM is used because it is not easy to compute the small strain stiffness of granular materials for varying interparticle friction angle experimentally. A numerical sample consisting of 9826 spheres similar to dry Grade chrome steel balls was prepared numerically. The sample was then subjected to shear for varying interparticle friction angle ranging from 1 to 50 degrees. The stress-strain behavior obtained from the numerical simulation was compared with the experimental results to warrant the validity of the simulation. The small strain stiffness was computed for varying interparticle friction angle and a relationship between the friction angle and small strain stiffness was established. It is noted that small strain stiffness is a function of interparticle friction angle for its lower value.

Keywords: *Small strain stiffness, interparticle friction, granular materials, discrete element method.*

1. INTRODUCTION

Interparticle friction angle is a dominant parameter that controls the mechanical behaviour of granular materials such as sand. The interparticle friction angle can be defined with the help of Figure 1, where f_n indicates the normal force exerted on the contact points between two particles, f_s indicates the shear force developed at the contact points between two particles, f indicates the force exerted on the contact points between two particles and ϕ indicates the interparticle friction angle. Experimentally, the effect of interparticle friction angle was reported by Skinner (1969). By shearing a random assembly of spherical particles, he depicted that both the effective angle of shearing resistance at constant volume and at peak stress state for a given initial porosity do not increase monotonically with the increase of the interparticle friction angle. Numerical studies using the particulate approach depicted that the characteristics of grain-scale level responses are severely affected by the interparticle friction angle (e.g., Hu & Molinary, 2004; Sazzad & Islam, 2008; Sazzad & Suzuki, 2011). The stability of a system depends on the values of the interparticle friction angle. A dense sample can behave like a loose sample for lower values of interparticle friction angle and can behave even like a fluid when the interparticle friction angle is almost zero (Sazzad & Islam, 2008). It was also reported that the macro-scale behaviors were significantly influenced by the variation of interparticle friction angle, in particular, at peak stress state (Sazzad et. al., 2017). Since the deformation properties of granular materials at small strain levels play an important role in predicting the short-term residual deformation of the ground and structural displacement, it is intended to study the macroscopic response at a very small strain level (lesser than 0.001%) due to the variation of interparticle friction angle. Earlier studies reported that the soil behavior observed by applying many small unload/reload cycles of axial stress statically in the laboratory tests is linear (e.g., Tatsuoka, Iwasaki, Fukushima & Sudo, 1979; Enomoto, 2016). It should be noted that the experimental device should be extremely precise with a higher degree of accuracy to measure the small strain stiffness. Conventional experimental facilities may not be able to measure the strain at such a very small strain level. Numerical methods such as the discrete element method (DEM) pioneered by Cundall and Strack (1979) can be used instead. So far, only a limited number of studies were reported in the literature that considered the DEM to estimate the small strain stiffness parameters (Sazzad et. al., 2017).

So, the objective of the present study is firstly to simulate the laboratory stress-strain response of conventional triaxial compression (CTC) tests carried out using the steel balls (i.e. spheres) and secondly to observe the effect of the variation of interparticle friction angle on the small strain stiffness parameter (i.e elastic modulus) of granular materials. To do this, the laboratory based conventional triaxial compression (CTC) test reported in Cui, O'Sullivan & O'Neil (2007)] and O'Sullivan, Cui & O'Neil (2008) on dry grade chrome steel balls under vacuum confinement of 80 kPa was simulated using the discrete element method. A numerical sample consisting of 9826 spheres was randomly generated without any initial interparticle contact. The generated numerical sample was compressed in different stages to attain a confining pressure of 80 kPa. During the compression, the periodic boundary condition was applied. The simulation of the CTC test was carried out under the strain control condition using the DEM. A very small strain increment was assigned so that the quasi-static condition could be attained and the effect of numerical damping became minimum. The simulated data were recorded at required intervals for the post analysis. The stiffness parameter at a very small strain range smaller than 0.001% was carefully measure for varying interparticle friction angle.

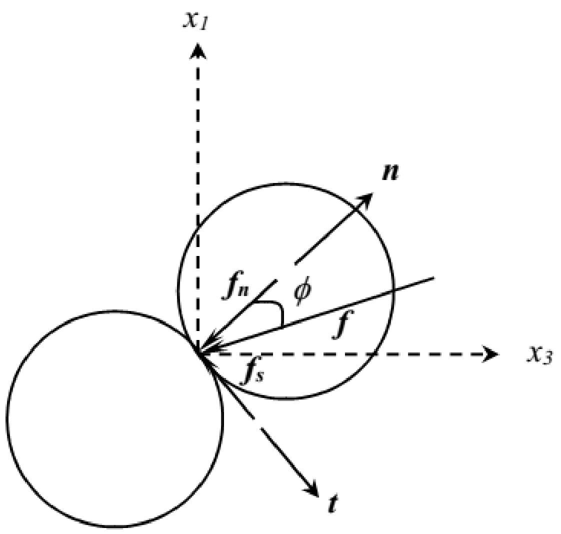

Figure 1: Interparticle friction angle, ϕ with force vectors in x_1-x_3 plane

2. DISCRETE ELEMENT METHOD AND OVAL

Discrete element method (DEM), also called distinct element method, is a family of numerical methods for computing the motion of large number of small particles. DEM is a numerical technique where Newton's second law of motion is applied. The translational and rotational accelerations of a 3D particle in DEM are computed using the Newton's second law of motion and are expressed as follows:

$$m\ddot{x} = \Sigma f_i \qquad i = 1-3 \tag{1}$$

$$I\ddot{\theta} = \Sigma M \tag{2}$$

where f_i are the force components, M is the moment, m is the mass, I is the moment of inertia, $\ddot{x}_i$ are the translation acceleration components and $\ddot{\theta}$ is the rotational acceleration of the particle. Velocities and displacements of particles are obtained by integrating the accelerations over time successively. For basics of DEM, readers can refer to Cundall and Strack (1979). Computer program OVAL is used to analyse the particulate assemble using the DEM. The effectiveness of OVAL has already been recognized (Kuhn, 1999; Sazzad & Suzuki, 2010; Sazzad & Suzuki, 2013; Sazzad, 2014). In the present study, Hertz-Mindlin contact model is used. The normal force of a Hertz-type contact is computed as follows (Sazzad, Sneha, & Rouf, 2017):

$$F^n = \frac{\bar{E}a^3}{R} \tag{3}$$

$$\bar{E} = \frac{8G}{3(1-\nu)} \tag{4}$$

$$a = \sqrt{\frac{d \times R}{2}} \tag{5}$$

$$R = \frac{2R_1R_2}{R_1 + R_2} \tag{6}$$

Here, $\bar{E}$ is the elastic constant, a is the contact radius, d is the overlap between the contacting particles, R is the effective radius of curvature, R_1 and R_2 are the radii of curvatures of two particles at contact.

3. NUMERICAL SAMPLE PREPARATION

In the present study, the laboratory based conventional triaxial compression (CTC) test reported in Cui, O'Sullivan & O'Neil (2007) and O'Sullivan, Cui & O'Neil (2008) on dry grade chrome steel balls under vacuum confinement of 80 kPa was used to compare with that of DEM to depict the authentication of DEM based simulated results. Three types of spheres having the radii of 2 mm, 2.5 mm and 3 mm, respectively, having a mixing ratio of each type particle of 1:1:1 (a sample height to width ratio of two) were used in the laboratory test. The void ratio of nonuniform sample used in the experiment was 0.603. The characteristics of the spheres used in the CTC tests as reported in Cui, O'Sullivan & O'Neil (2007) and O'Sullivan, Cui & O'Neil (2008) are shown in Table 1. For numerical study, a numerical sample consisting of 9826 spheres similar to the experimental study was randomly generated without any initial contacts among spheres. The spheres were modeled as particles. This is because it simplifies the contact detection algorithm and thus, it reduces the computational cost of the simulation. The radii of spheres used to make the numerical samples were same as the experiment (i.e. 2 mm, 2.5 mm and 3 mm), respectively with a mixing ratio of 1:1:1. The initial sample is surrounded by the periodic boundaries, a boundary condition in which the periodic cells are surrounded by the identical cells. The generated numerical sample was compressed in different stages to attain a confining pressure of 80 kPa. The consolidation of the initially generated sparse sample was carried out using the strain control condition. After the end of isotropic compression, the void ratio of the numerical sample became 0.626. The void ratio of the numerical sample is a bit higher than that of the experiment. However, it is expected that this very small difference of the void ratio between the experiment and numerical sample has very little effect on the shear behavior.

Table 1: Characteristics of dry grade chrome steel balls used in the CTC test (after Cui, O'Sullivan & O'Neil 2007)

Properties	Values
Density of spheres (kg/m^3)	7.8 ×10^3
Shear modulus (Pa)	7.9 ×10^3
Poisson's ratio	0.28
Interparticle friction angle (degree)	5.5
Boundary friction coefficient	0.228

4. NUMERICAL SIMULATIONS

The simulation of the CTC test was carried out under the strain control condition using DEM. A very small strain increment was assigned during shear. The material properties and DEM parameters used in the simulation are shown in Table 2. It should be noted that the properties of particles used in DEM simulation are same as that of grade chrome steel balls used in the experiment (CTC test). To monitor the quasi-static condition, a non-dimensional index is defined as follows (Sazzad, Sneha, & Rouf, 2017; Sazzad, 2014):

$$I_{uf} = \sqrt{\frac{\sum_{1}^{N_p} F_{ubf}^2 / N_p}{\sum_{1}^{N_c} F^2 / N_c}} \times 100\,(\%) \tag{7}$$

where F_{ubf} , F , N_p and N_c denote the unbalanced force, contact force, number of particles and number of contacts, respectively. Index I_{uf} is directly related to the accuracy of the simulation. Lower the value of I_{uf} , higher the accuracy of the simulation.

Table 2: Material properties and DEM parameters used in the present study

Properties	Values
Density of spheres (kg/m^3)	7.8 ×10^3
Shear modulus (Pa)	7.9 ×10^3
Poisson's ratio	0.28
Interparticle friction angle (degree)	1 to 50
Increment of time step (s)	1.0 ×10^{-6}
Damping coefficients	0.10

5. VALIDATION OF SIMULATED RESULTS

The simulation of the CTC test was carried out under the strain control condition using DEM. The Simulated stress-strain behavior is compared with the laboratory CTC test as reported in Cui, O'Sullivan & O'Neil (2007) and depicted in Figure 2 The normalized deviatoric stress, q in Figure 2 is defined as $q = (\sigma_1 - \sigma_3)/\sigma_3$, σ_1 and σ_3 are the stresses in vertical and lateral directions, respectively. It is noted that the stress-strain behavior by DEM has excellent agreement with the laboratory CTC test reported in Cui, O'Sullivan & O'Neil (2007). This quantitative validation of the simulated results with the experiment depicts the versatile nature of the present study by DEM and proofs that DEM can successfully replicate the behavior of granular materials quantitatively.

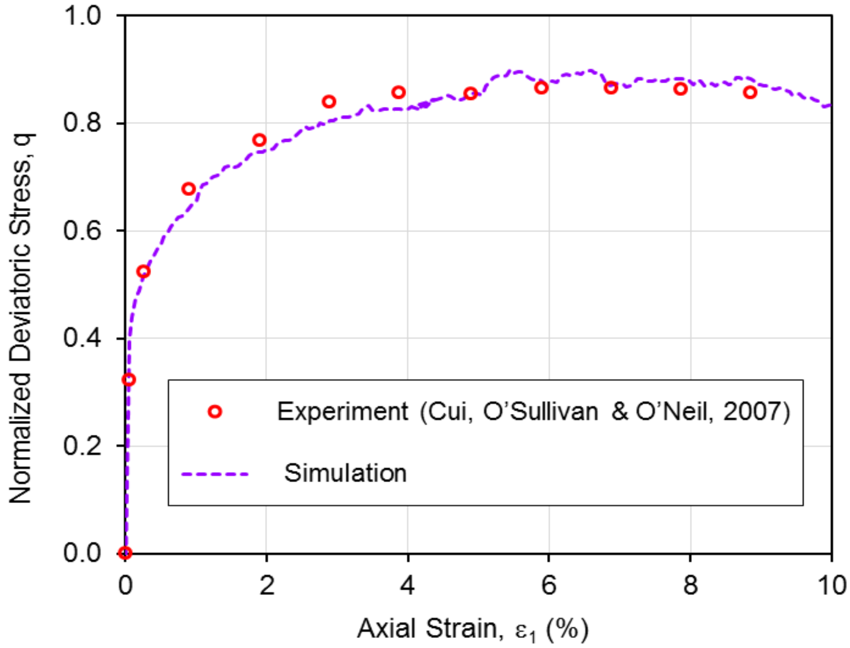

Figure 2: Comparison of the simulated stress-strain behavior using DEM with the experiment reported in Cui, O'Sullivan & O'Neil (2007)

6. EFFECT OF INTERPARTICLE FRICTION ANGLE

The effect of interparticle friction angle is studied in this section. For this reason, several CTC tests were simulated for varying interparticle friction angles ranging from 1 to 50 degrees. Figure 3 shows the stress-strain behavior of granular materials for three different interparticle friction angles (i.e. 5, 25 and 45 degrees) during shear. It is observed that the interparticle friction angle has severe effect on the stress-strain behavior. The peak stress increases with the increase of the interparticle friction angle. Same behavior is also reported in earlier DEM studies (Sazzad and Islam, 2008; Sazzad, Alam & Rowshan, 2017). The evolution of the volumetric strain with axial strain is depicted in Figure 4.

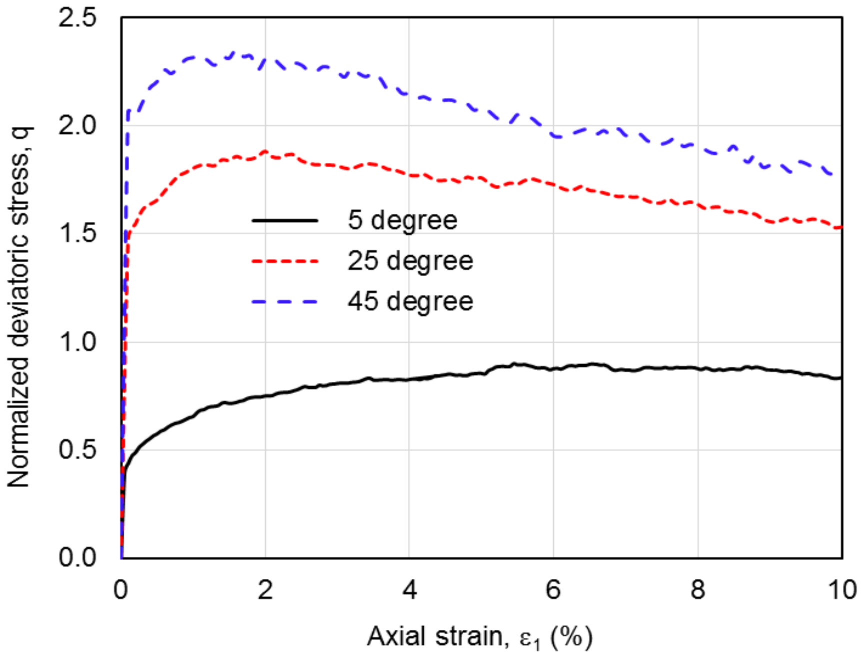

Figure 3: Stress-strain relationship for varying interparticle friction angle

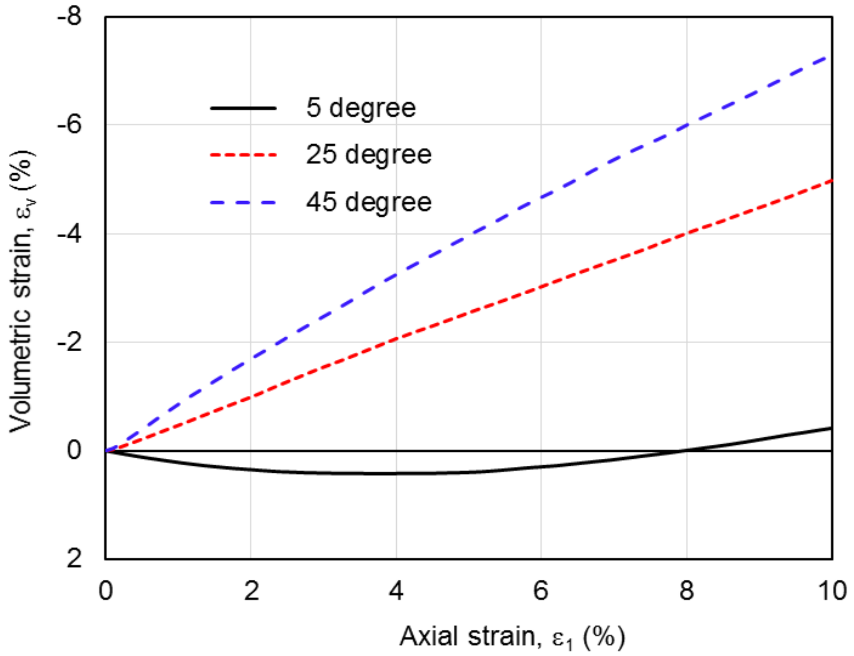

Figure 4: Evolution of volumetric strain for varying interparticle friction angle

The volumetric strain is defined as $\varepsilon_v = \varepsilon_1 + 2\varepsilon_3$, where ε_1 is the strain in x_1- direction and ε_3 is the strain in x_3- direction. The positive value of strain indicates compression while the negative value indicates dilation. It is observed that dilation of the sample increases with the increase of interparticle friction angle. The relationship between the elastic modulus and interparticle friction angle at small strain lower than 0.001% is depicted in Figure 5.

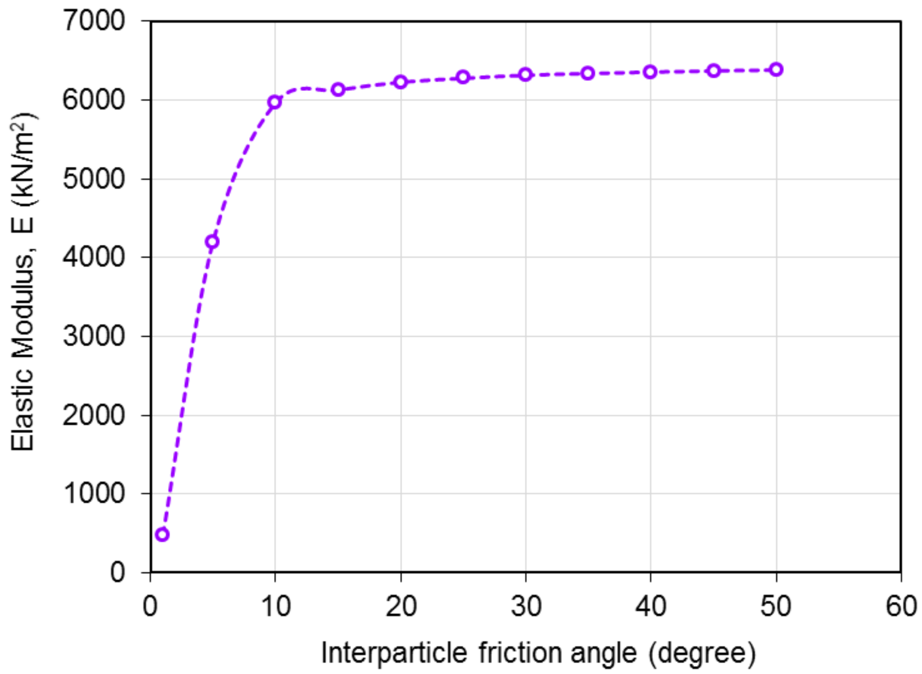

Figure 5: Relationship between the elastic modulus and interparticle friction angle at small strain range lower than 0.001%

The elastic modulus increases sharply with the increase of the interparticle friction angle up to 10 degree and beyond that the elastic modulus becomes almost constant with the further increase of interparticle friction angle. So, it can be concluded that elastic modulus is the function of the interparticle friction angle for the lower range of interparticle friction angle only.

7. CONCLUSIONS

This study simulated the stress-strain behavior of a numerical sample consisting of 9826 spheres similar to dry Grade chrome steel balls reported in Cui, O'Sullivan & O'Neil (2007). An excellent agreement between the simulated and experimental stress-strain behavior was observed. This illustrates the accuracy and perfectness of the simulation using DEM. The effect of the variation of the interparticle friction angle on the stress-strain-dilative behavior was investigated. It is observed that interparticle friction angle severely affects the stress-strain behavior at peak stress state. Peak stress increases with the increase of the interparticle friction angle. The dilation also increases with the increase of the interparticle friction angle. The stiffness parameter i.e. the elastic modulus is also calculated at a very at small strain range lower than 0.001%. The relationship between the elastic modulus and the interparticle friction angle is illustrated. It is noted that the value of elastic modulus increases with the increase of interparticle friction angle for lower values of interparticle friction angle. So it can be concluded that elastic modulus is the function of the interparticle friction angle for its lower value only.

REFERENCES

Cui, L., O'Sullivan, C., & O'Neil, S. (2007). An analysis of the triaxial apparatus using a mixed boundary three-dimensional discrete element model. *Geotechnique*, 57(10), 831–844.

Cundall, P.A. (1971). A computer model for simulating progressive, large scale movement in blocky rock systems. *Proc. Symp. Int. Soc. Rock Mech., Inst. Civ. Engrg*., 2(8), 129-136.

Enomoto, T. (2016). Effects of grading and particle characteristics on small strain properties of granular materials. *Soils and Foundations,* 56(4), 745–750.

Hu, N., & Molinari, J. F. (2004). Shear band in dense metallic granular materials. *Journal of Mechanics and Physics of Solids*, 52(3), 499-531.
Kuhn, M.R. (1999). Structured deformation in granular materials. *Mechanics of Materials*, 31(6), 407-429.
Mechanics and Physics of Solids, 52, 499-531
Mechanics and Physics of Solids, 52, 499-531
O'Sullivan, C., Cui, L., & O'Neill, S. (2008). Discrete element analysis of the response of granular materials during cyclic loading. *Soils and Foundations,* 48(4), 511-530.
Sazzad, M. M. & Islam, M. S. (2008). Macro and micro mechanical responses of granular material under varying interparticle friction. *Journal of Civil Engineering*. 36(2). 87-96.
Sazzad, M. M. & Suzuki, K. (2010). Micromechanical behavior of granular materials with inherent anisotropy under cyclic loading using 2D DEM. *Granular Matter*, 12(6), 597–605.
Sazzad, M. M. & Suzuki, K. (2011). Effect of Interparticle Friction on the Cyclic Behavior of Granular Materials Using 2D DEM. *Journal of Geotechnical and Geoenvironmental Engineering*, ASCE, 137(5). 545-549.
Sazzad, M. M. & Suzuki, K. (2013). Density dependent macro-micro behavior of granular materials in general triaxial loading for varying intermediate principal stress using DEM. *Granular Matter*, 15(5), 583-593.
Sazzad, M. M. (2014). Micro-scale behavior of granular materials during cyclic loading. *Particuology*, 16, 132–141, 2014.
Sazzad, M.M., Alam, A.A., & Rowshan, M.N.A. (2017). Effect of interparticle friction angle on the stress-dilatancy responses of granular materials by DEM. *Journal of Engineering Science*, 8(1), 41-50.
Sazzad, M.M, Islam, M.S., & Hossain, M.S. (2017). Measurement of Small Strain Stiffness Parameters of Granular Materials. *International Conference on Mechanical, Industrial and Materials Engineering*, RUET, Rajshahi, Bangladesh.
Sazzad, M.M., Sneha, E., & Rouf, R.B. (2017). Comparison of stress-stain behavior of CTC test using DEM simulation. *International Conference on Planning, Architecture and Civil Engineering*, Rajshahi, Bangladesh, 194-199.
Skinner, A.E. (1969). A note on the influence of interparticle friction on the shearing strength of a random assembly of spherical particles. *Geotechnique*, 19(1), 150-157.
Tatsuoka, F., Iwasaki, T., Fukushima, S., & Sudo, H. (1979). Stress conditions and stress histories affecting shear modulus and damping of sand under cyclic loading. Soils and Foundation, 19(2), 29–43.